ACS Macro Letters

Letter

pubs.acs.org/macroletters

All Organic Nanofibers As Ultralight Versatile Support for Triplet–Triplet Annihilation Upconversion

Christian Wohnhaas,[†] Kathrin Friedemann,[†] Dmitry Busko,[†] Katharina Landfester,[†] Stanislav Baluschev,[†,‡] Daniel Crespy,*[,†] and Andrey Turshatov*[,†]

[†]Max Planck Institute for Polymer Research, Ackermannweg 10, 55128 Mainz, Germany

[‡]Optics and Spectroscopy Department, Faculty of Physics, Sofia University "St. Kliment Ochridski", James Bourchier 5, 1164 Sofia, Bulgaria

Supporting Information

ABSTRACT: We present a method for the fabrication of ultralight upconverting mats consisting of rigid polymer nanofibers. The mats are prepared by simultaneously electrospinning an aqueous solution of a polymer with pronounced oxygen-barrier properties and functional nanocapsules containing a sensitizer/emitter couple optimized for triplet–triplet annihilation photon upconversion. The optical functionality of the nanocapsules is preserved during the electrospinning process. The nanofibers demonstrate efficient upconversion fluorescence centered at λ_{max} = 550 nm under low intensity excitation with a continuous wave laser (λ = 635 nm, power = 5 mW). The pronounced oxygen-barrier property of the polymer matrix may efficiently prevent the oxygen penetration so upconversion fluorescence is registered in ambient atmosphere. The demonstrated method can be used for the production of upconverting ultralight porous coatings for sensors or upconverting membranes with freely variable thickness for solar cells.

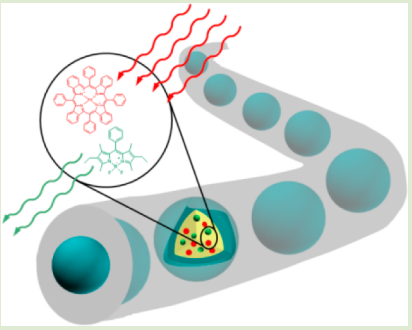

The process of generation of photons with higher energy under excitation by photons with lower energy is known as photon upconversion (UC). Triplet–triplet annihilation upconversion (TTA-UC) was reported in the early 60's of the last century (the process was called p-type delayed fluorescence)[1] but attracted much attention only in the past decade. In contrast to other upconversion techniques such as two-photon absorption,[2] second harmonic generation,[3] sequential energy transfer, or excited-state absorption in rare earth ion-doped inorganic glasses,[4] the fundamental advantage of the TTA-UC is the very low intensity (~several mW cm^{-2}) and the extremely low spectral power density (as low as ~100 μW nm^{-1}) of the excitation source, that might correspond to the intensity of low concentrated sunlight.[5,6] The excitation band for efficient TTA-UC can be gradually extended from blue to NIR regions of the optical spectra.[7−16] TTA-UC quantum yield can reach over 10%[17−19] under certain conditions, which makes the process attractive for applications in material science and medicine. The unique opportunities of TTA-UC have been exploited in areas of solar energy conversion,[20] photocatalysis,[21] and bioimaging.[22,23]

The typical UC-system consists of two types of organic dyes: a sensitizer (usually metalated macrocycles, with a high value of intersystem crossing (ISC) coefficient) and an emitter (aromatic hydrocarbons with a very low ISC-coefficient) dissolved in an organic solvent. The dyes used in this work are shown in Figure 1: sensitizer, meso-tetraphenyl-tetrabenzo-porphyrin palladium (PdTBP), and emitter, 1,3,5,7-tetramethyl-8-phenyl-2,6-diethyl dipyrromethane·BF_2 (dye550). The process of TTA-UC is performed in agreement with the simplified scheme presented in Figure 1. First, after absorption of light (λ = 635 nm) by the sensitizer, through the process of ISC a long-lived sensitizer triplet state is formed. Then, four types of relaxation are possible: (i) the energy of sensitizer triplet state can be transferred to an emitter triplet state by the process of triplet–triplet transfer (TTT); (ii) a phosphorescent photon can be emitted; (iii) the excited triplet state can be quenched by molecular oxygen or other quenchers; and (iv) the triplet state can relax in a nonradiative manner. The populated emitter triplet state through the scenario (i) demonstrates very long lifetime, because the ISC in the emitter is a strongly forbidden process (the ISC-coefficient of the emitter molecules is negligible). Thus, there are only two possibilities for further energy dissipation: triplet–triplet annihilation (TTA) or quenching the emitter triplet state by a molecule of oxygen or other quenchers. In the TTA process, one of the excited emitter triplet returns to the ground state, but the other molecule accumulates the total energy of the two triplets and populates the excited singlet state. Finally, the excited molecule emits a photon (λ_{max} = 550 nm) with a wavelength much shorter than the wavelength of the photons initially absorbed. There are several crucial factors that affect the efficiency of the TTA-UC: first, the efficiency of the TTT is determined by the overlap of the sensitizer and emitter triplet

Received: February 28, 2013
Accepted: April 26, 2013
Published: May 6, 2013

   dx.doi.org/10.1021/mz400100j | *ACS Macro Lett.* 2013, 2, 446−450

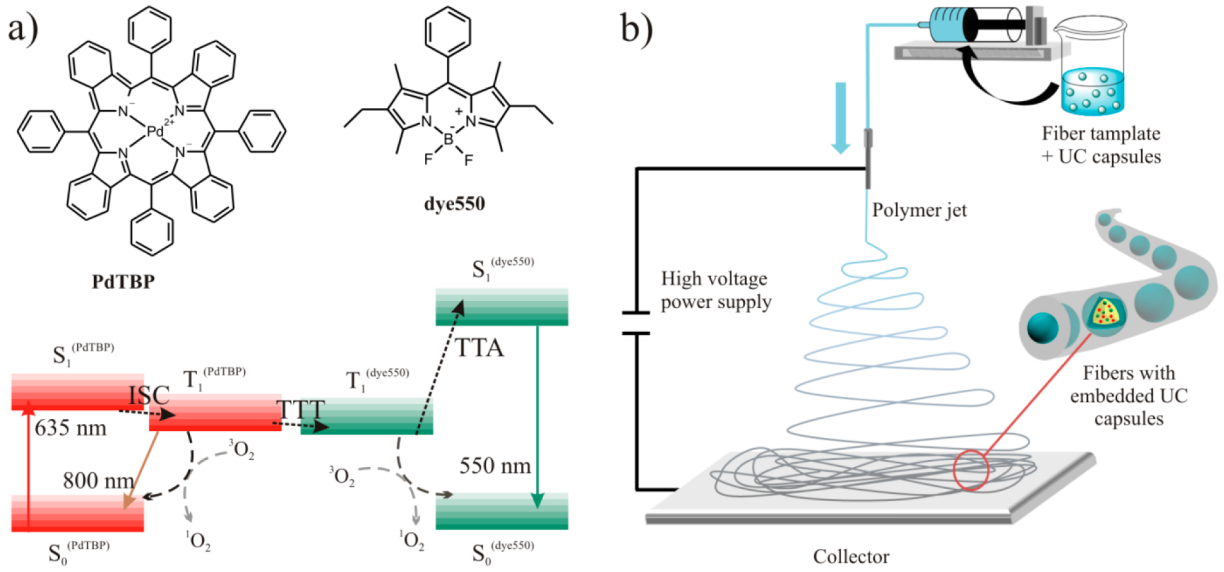

Figure 1. (a) Simplified energetic schema of the TTA-UC process. Excitation wavelength λ = 635 nm (Q-band of the sensitizer, PdTPB), residual sensitizer phosphorescence at λ_{max} = 800 nm, and UC-fluorescence at λ_{max} = 550 nm (emitter, dye550); (b) Schematics of the colloid-electrospinning process for embedding UC nanocapsules in nanofibers.

manifolds.[7,9] Second, both processes, TTT and TTA, depend strongly on the viscosity of the matrix, that is, the organic solvent. The increase of viscosity leads to substantial decrease of the efficiency of the TTT[24] and TTA.[25] However, if the dye concentration is sufficiently high (~100s mM), ultra-long-range excited-state energy transfer is possible.[26] Thus, TTA-UC may occur even in rigid matrices, although with a low efficiency.

Finally, because the mechanism of TTA-UC includes energy exchange between the triplet states of the sensitizer and the emitter, the UC efficiency is extremely sensitive to presence of molecular oxygen. There are several successful examples where issues of dye mobility and oxygen quenching were separately or simultaneously solved. Efficient TTA-UC has been reported in the solid state.[27] The thin films were composed of metalated porphyrin macrocycles blended in a matrix of blue emitting polymers such as polyfluorenes[28] and polypentaphenylenes.[29] TTA-UC was demonstrated in films of poly(methyl methacrylate)[30] or cellulose acetate,[31] and rubbery host polymers.[8,32,33] Incorporation of the hydrophobic UC-dyes in water-soluble carriers enables a range of unique applications in the fields of material- and life-science. Efficient TTA-UC operating in aqueous environment, with the UC-dyes loaded into micelles,[34] nanoparticles,[23,35,36] nanocapsules,[22] and microcapsules[37] was shown.

In our previous work[22] we encapsulated the nonvolatile organic solvent (hexadecane) dissolving the UC-dyes in polymer nanocapsules. TTA-UC system being in water phase sustained all properties of UC process that were demonstrated in organic solutions. Nevertheless, the nanocapsules dispersed in water could not be directly used in coatings, films, or any solid matrix due to weak shell durability. Among the available type of materials, nanofibers fabricated by electrospinning have the advantage to be ultralight, scalable, and can be produced from a large variety of polymers.[38−43] Colloid-electrospinning offers a unique combination of remarkable features of both nanoparticles and nanofibers, that is, high surface area, ultralight weight because of the macroscopic porous structures, and possibility to deposit additional materials on the surface and handle them in the form of fibers.[44] Thus, polymer[45−47] and inorganic[48−50] nanoparticles were electrospun separately or simultaneously[51] to yield nanostructured fibers. Recently, electrospun fibers were used to embed upconverting inorganic nanoparticles,[52,53] thylakoid vesicles,[54] microparticles for the release of a pheromone,[55] and capsules containing hexadecane for thermal energy storage.[56] In our experiment, nanofibers fabricated by electrospinning were investigated as platform for nanocapsules synthesized by the emulsion-solvent evaporation process[57] and demonstrating TTA-UC. Additionally, the electrospinning of nanocapsules offered a possibility to double-encapsulate the TTA-UC agents. Indeed, since a polymer matrix is needed to provide the viscoelastic forces necessary to allow a continuous jet to be formed, we chose to select a polymer known for its oxygen barrier properties, that is, poly(vinyl alcohol) (PVA). Indeed, the permeation coefficient of some PVA films was reported to be 0.09 cm^3 mm m^{-2} day^{-1} atm^{-1} at 24 °C and 75% relative humidity.[58] For instance, PVA was found to be an excellent oxygen-barrier for solar cells.[59] The PVA matrix hence served to immobilize and to protect the nanocapsules and TTA-UC chemical agents. This novel approach allows performing TTA-UC in rigid ultralight materials.

Because evaporation of the solvents and water from the jet occurs during the electrospinning process, 1-phenylheptadecane (PHD) was chosen as a solvent with very high boiling point to dissolve the UC-dyes. For the preparation of nanocapsules, the dyes for TTA-UC and a polymer, either poly(methyl methacrylate) (NC1) or a polystyrene-*block*-poly(methyl methacrylate) (NC2), were dissolved in a mixture of a solvent (chloroform) and a hydrophobic liquid with high boiling point (PHD), and subsequently emulsified in an aqueous medium. After evaporation of the solvent, nanocapsules with PHD core dispersed in water were obtained. As shown in Figure 2a,b, well-defined core−shell structures could be identified by TEM. Nanocapsules of two different sizes (~110 nm for NC1 and ~136 nm for NC2) could be successfully prepared with uniform and narrow size distribution (Table 1). Figure 2c displays typical luminescence spectra measured from NC1 and NC2 nanocapsules dispersed in

dx.doi.org/10.1021/mz400100j | ACS Macro Lett. 2013, 2, 446−450

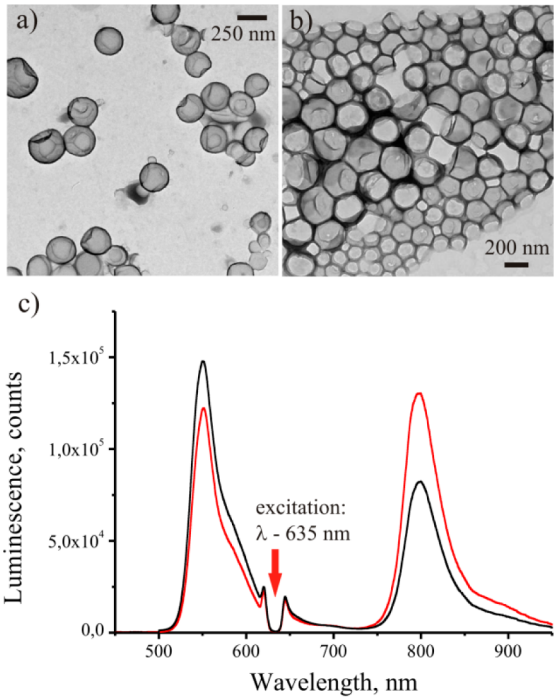

Figure 2. TEM micrographs of (a) the NC1 nanocapsules, (b) the NC2 nanocapsules; (c) black line, luminescence spectra for water dispersion of NC1 nanocapsules ($C_{PdTBP} = 1 \times 10^{-3}$ mol L^{-1}/$C_{dye550} = 1 \times 10^{-2}$ mol L^{-1} in the PHD); red line, NC2 nanocapsules ($C_{Pd\text{-}TBP} - 1 \times 10^{-3}$ mol L^{-1}/$C_{dye550} = 1 \times 10^{-2}$ mol L^{-1} in the PHD). Both samples were sealed in a glovebox with an oxygen concentration below 2 ppm.

Table 1. Characteristics of Fabricated Nanofibers

fiber	capsules	$R_{h\ capsules}$ (nm)	D_{fibers}[a] (nm)
NF1	NC1	110 ± 21	269 ± 59
NF2	NC1	110 ± 21	462 ± 87
NF3	NC2	136 ± 50	328 ± 28
NF4	NC2	136 ± 50	482 ± 116

[a]Determined by ImageJ analysis of SEM micrographs.

deoxygenated aqueous media (4% w/w concentration of dispersed phase) at room temperature. Strong UC fluorescence of dye550 at λ_{max} = 550 nm and residual phosphorescence of PdTBP at λ_{max} = 800 nm were observed. Luminescence spectra measured in an ambient atmosphere are presented in the Supporting Information (Figure S1).

Nanocapsules were electrospun in PVA nanofibers with average diameters comprised between 250 and 500 nm (Table 1). The SEM micrographs revealed that the fibers displayed a relatively homogeneous thickness and a smooth surface (Figure 3a,d).

For the localization and distribution of the nanocapsules in the fibers, confocal laser scanning microscopy (CLSM) was applied by using direct excitation of the emitter (here dye550), as shown in Figure 2b. The emitter was excited with a wavelength λ_{exc} = 488 nm and the collected emitted light was detected in the interval $\Delta\lambda_{det}$ = 500−550 nm. As shown in Figure 2b, the nanocapsules were homogeneously distributed in the fibers. Some holes were observed by SEM on the nanofibers surface due to the capsule opening induced by the vacuum in the SEM chamber.

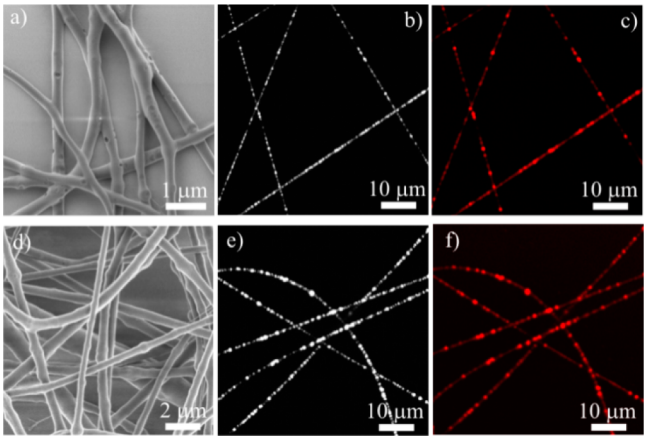

Figure 3. SEM micrographs of NF1 fibers (a) and NF4 fibers (d); CLSM micrographs of NF1 fibers (b) direct excitation (λ_{exc} = 488 nm, $\Delta\lambda_{det}$ = 500−550 nm); (c) UC excitation (λ_{exc} = 633 nm, $\Delta\lambda_{det}$ = 500−550 nm); CLSM micrographs of NF4 fibers (e) direct excitation (λ_{exc} = 488 nm, $\Delta\lambda_{det}$ = 500−550 nm); (f) UC excitation (λ_{exc} = 633 nm, $\Delta\lambda_{det}$ = 500−550 nm). All CLSM measurements were carried out in an ambient atmosphere at room temperature.

Bright UC-fluorescence was detected (Figure 3c,f) in an ambient atmosphere, without any further protection of the sample regarding the molecular oxygen. The images demonstrated in Figure 3c,f were obtained in UC-excitation regime, namely, excitation in the Q-band of the sensitizer (λ_{exc} = 633 nm). The emitted light was collected in the same spectral interval $\Delta\lambda_{det}$ = 500−550 nm (overlapping with the spectral interval for direct excitation of the emitter).

To verify that TTA-UC fluorescence occurred, monotonic tuning of the central wavelength of the registration window was performed. Controlling the parameters of the adjustable diffraction slits, the central wavelength was increased with a step of $\delta\lambda_{det}$ = 5 nm (with 10 nm detection bandwidth). It is important to notice that the same area of the sample was scanned sequentially and the emitted light was detected in the range $\Delta\lambda_{det}$ = 500−575 nm. The results of the detection interval scanning are presented in Figure 4a.

An UC-fluorescence maximum (λ_{max} = 541 nm) in diluted toluene solution of the same dye was previously reported.[60] The maximum of TTA-UC fluorescence (λ_{max} = 550 nm, Figure 2c) measured in water dispersion of the same

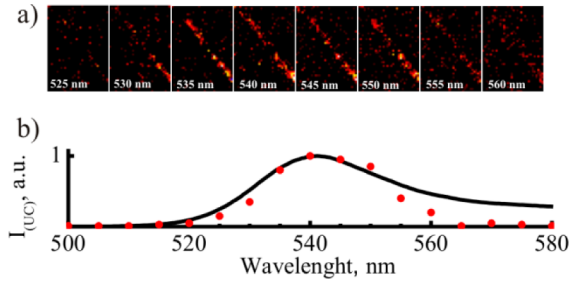

Figure 4. (a) Sequential CLSM-images of a fiber NF1 by tuning of the detection interval. Excitation at λ_{exc} = 633 nm (excitation power 0.3 μW); overall detection interval, $\Delta\lambda_{det}$ = 500−575 nm. (b) Normalized fluorescence spectrum of dye550 in toluene (black line), fluorescent spectra recovered by the analysis of the CLSM images in (a) (red dots). CLSM measurements were carried out in an ambient atmosphere at room temperature.

dx.doi.org/10.1021/mz400100j | ACS Macro Lett. 2013, 2, 446−450

nanocapsules (NF1) was slightly red-shifted compared to the fluorescence of dye550 in toluene, mostly due to the self-absorption caused by the higher dye concentration in the nanocapsules. The brightest CLSM signal was detected in the interval 530−545 nm, coinciding with the emission maximum of the dye550. This fact proves once again that the fluorescence of dye550 was observed under UC-excitation regime. It is important to note that the fluorescent signal decreases drastically when λ_{det} > 560 nm. Therefore, a very common artifact due to scattered light can be totally excluded. Another artifact, two-photon excitation of dye550 by the laser irradiation at λ = 633 nm and used light intensity (in order of 100 W cm^{-2}), could be excluded too: neither blank nanocapsules nor toluene solutions of dye550 fluoresce, if prepared in the absence of the triplet sensitizer.

Incorporating nanocapsules into the PVA fibers provides an additional function. Indeed, PVA may improve the protection of TTA-UC nanocapsules from the destructive influence of molecular oxygen. The discovery of materials for upconversion in ambient atmosphere showing efficiency comparable with the one displayed in oxygen-free conditions is an important aim. We fabricated fibers with various thicknesses by changing the electrospinning parameters. All fabricated fibers (NF1-NF4) showed upconversion, even without any deoxygenating step. SEM and CLSM micrographs of nanofibers NF2 and NF3 are presented in the Supporting Information (Figures S2,S3). We compared the UC-fluorescence of fibers sealed in oxygen-free conditions (nitrogen filled glovebox) and fibers left under air. Micrographs obtained with CLSM are presented in the Supporting Information (Figure S4). We did not observe significant differences in UC intensity between the fibers sealed in the glovebox (oxygen free conditions) and the fibers maintained in the ambient atmosphere for similar parameters of image acquisition. Thus, quenching of UC-emission by molecular oxygen was successfully reduced. The samples were able to demonstrate efficient UC-fluorescence after at least one month from the moment of fabrication, even when stored in ambient conditions. This fact opens additional perspectives in the fabrication of new UC nanomaterials. Larger amount of fibers in the form of a macroscale mat (Figure 5a) could be produced by electrospinning for a longer time (under electrospinning conditions corresponding to NF2 fibers).

The lightweight fiber mat exhibited UC-fluorescence that was detectable by naked eye (Figure 5a). The mat demonstrated an absence of dye photobleaching when the intensity of the incident light was below ∼136 mW cm^{-2} (Figure 5b). However, a significant decrease of UC fluorescence occurred after several minutes of continuous irradiation under stronger light irradiation (>276 mW cm^{-2}).

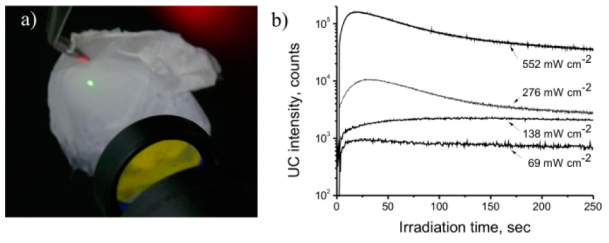

Figure 5. (a) Photograph of a fiber mat under illumination of a HeNe laser (λ = 633 nm, laser power = 5 mW, light intensity ∼ 500 mW cm^{-2}). The green dot in the center is UC-fluorescence. The notch filter was used in order to suppress the scattered laser light. (b) Changes of UC fluorescence (at λ_{max} = 550 nm) under continuous irradiation of the fiber mat at different power of incident light (λ = 635 nm). All measurements were carried out in ambient atmosphere and room temperature.

In summary, the high viscosity of the matrix containing upconverting materials and the quenching by molecular oxygen are parameters, which limit the efficiency of the TTA-UC process. Our approach is to create core−shell nanoparticles containing the active dyes for TTA-UC dissolved in the liquid core in order to preserve their mobility. The polymer shell prevents coalescence between the droplets of liquid cores and allows therefore the processability of the functional nanocapsules by electrospinning. The obtained ultralight nanostructured mats consist of rigid polymer nanofibers and embedded nanocapsules, without loss of the nanocapsules UC-functionality. The illumination of the mats with a red laser yielded a strong fluorescence at λ_{max} = 550 nm. The UC-efficiency in oxygen-free and aerobic conditions is comparable. This simple method allows therefore the elaboration of a wide variety of upconverting structures since the mats could be deposited virtually on any surface. Because the thickness of the mats can be controlled by the electrospinning time, the applications range from biosensing in the case of the electrospinning of few nanofibers to applications in solar energy conversion for thicker membranes.

■ ASSOCIATED CONTENT

Supporting Information

Contains supplementary table, figures, and experimental details on UC nanocapsules formation, electrospinning, TEM, SEM, CLSM, and instrumentation for UC measurements. This material is available free of charge via the Internet at http://pubs.acs.org.

■ AUTHOR INFORMATION

Corresponding Author

*E-mail: turshat@mpip-mainz.mpg.de; crespy@mpip-mainz.mpg.de.

Notes

The authors declare no competing financial interest.

■ ACKNOWLEDGMENTS

A.T. acknowledges the EU-founded FP-7 project EphoCell (N 227127) for the financial support, and S.B. acknowledges the Reintegration Grant RG-09-0002 (DRG-02/2) Bulgarian National Science Fund for the financial support.

■ REFERENCES

(1) Parker, C. A.; Hatchard, C. G. *Proc. R. Soc. London* **1962**, *14*, 386−387.
(2) Denk, W.; Strickler, J. H.; Webb, W. W. *Science* **1990**, *248*, 73−76.
(3) Boyd, R. W. *Nonlinear Optics*, 3rd ed.; Academic Press: New York, 2008.
(4) Haase, M.; Schäfer, H. *Angew. Chem., Int. Ed.* **2011**, *50*, 5808−5829.
(5) Baluschev, S.; Miteva, T.; Yakutkin, V.; Nelles, G.; Yasuda, A.; Wegner, G. *Phys. Rev. Lett.* **2006**, *97*, 143903.
(6) Miteva, T.; Yakutkin, V.; Nelles, G.; Baluschev, S. *New J. Phys.* **2008**, *10*, 103002.
(7) Baluschev, S.; Yakutkin, V.; Miteva, T.; Avlasevich, Y.; Chernov, S.; Aleshchenkov, S.; Nelles, G.; Cheprakov, A.; Yasuda, A.; Müllen, K. *Angew. Chem., Int. Ed.* **2007**, *46*, 7693−7696.

(8) Islangulov, R. R.; Lott, J.; Weder, C.; Castellano, F. N. *J. Am. Chem. Soc.* **2007**, *129*, 12652−12653.
(9) Baluschev, S.; Yakutkin, V.; Wegner, G.; Miteva, T.; Nelles, G.; Yasuda, A.; Chernov, S.; Aleshchenkov, S.; Cheprakov, A. *Appl. Phys. Lett.* **2007**, *90*, 181103−181103−3.
(10) Singh-Rachford, T. N.; Haefele, A.; Ziessel, R.; Castellano, F. N. *J. Am. Chem. Soc.* **2008**, *130*, 16164−16165.
(11) Singh-Rachford, T. N.; Castellano, F. N. *J. Phys. Chem. A* **2008**, *112*, 3550−3556.
(12) (a) Yakutkin, V.; Aleshchenkov, S.; Chernov, S.; Miteva, T.; Nelles, G.; Cheprakov, A.; Baluschev, S. *Chem.—Eur. J.* **2008**, *14*, 9846−9850. (b) Miteva, T.; Yakutkin, V.; Nelles, G.; Baluschev, S. *New J. Phys.* **2008**, *10*, 103002.
(13) Singh-Rachford, T. N.; Castellano, F. N. *J. Phys. Chem. A* **2009**, *113*, 5912−5917.
(14) Ji, S.; Wu, W.; Wu, W.; Guo, H.; Zhao, J. *Angew. Chem., Int. Ed.* **2011**, *50*, 1626−1629.
(15) Singh-Rachford, T. N.; Castellano, F. N. *J. Phys. Chem. Lett.* **2010**, *1*, 195−200.
(16) Wu, W.; Guo, H.; Wu, W.; Ji, S.; Zhao, J. *J. Org. Chem.* **2011**, *76*, 7056−7064.
(17) Cheng, Y. Y.; Khoury, T.; Clady, R. G.; Tayebjee, M. J.; Ekins-Daukes, N.; Crossley, M. J.; Schmidt, T. W. *Phys. Chem. Chem. Phys.* **2009**, *12*, 66−71.
(18) Cheng, Y. Y.; Fückel, B.; Khoury, T.; Clady, R. l. G.; Tayebjee, M. J.; Ekins-Daukes, N.; Crossley, M. J.; Schmidt, T. W. *J. Phys. Chem. Lett.* **2010**, *1*, 1795−1799.
(19) Khnayzer, R. S.; Harrington, J. A.; Haefele, A.; Deng, F.; Castellano, F. N. *Chem. Commun.* **2012**, *48*, 209−211.
(20) Schulze, T. F.; Czolk, J.; Cheng, Y.-Y.; Fückel, B.; MacQueen, R. W.; Khoury, T.; Crossley, M. J.; Stannowski, B.; Lips, K.; Lemmer, U. *J. Phys. Chem. C* **2012**, *116*, 22794−22801.
(21) Kim, J. H.; Kim, J. H. *J. Am. Chem. Soc.* **2012**, *134*, 17478−17481.
(22) Wohnhaas, C.; Turshatov, A.; Mailänder, V.; Lorenz, S.; Baluschev, S.; Miteva, T.; Landfester, K. *Macromol. Biosci.* **2011**, *11*, 772−778.
(23) Liu, Q.; Yang, T.; Feng, W.; Li, F. *J. Am. Chem. Soc.* **2012**, *134*, 5390−5397.
(24) Porter, G.; Wilkinson, F. *Proc. R. Soc. London* **1961**, *264*, 1−18.
(25) Borowicz, P.; Nickel, B. *J. Opt. Soc. Am. B* **2005**, *22*, 315−322.
(26) Ito, A.; Stewart, D. J.; Fang, Z.; Brennaman, M. K.; Meyer, T. J. *Proc. Natl. Acad. Sci. U.S.A.* **2012**, *109*, 15132−15135.
(27) Simon, Y. C.; Weder, C. *J. Mater. Chem.* **2012**, *22*, 20817−20830.
(28) Keivanidis, P. E.; Baluschev, S.; Miteva, T.; Nelles, G.; Scherf, U.; Yasuda, A.; Wegner, G. *Adv. Mater.* **2003**, *15*, 2095−2098.
(29) Baluschev, S.; Keivanidis, P.; Wegner, G.; Jacob, J.; Grimsdale, A. C.; Mullen, K.; Miteva, T.; Yasuda, A.; Nelles, G. *Appl. Phys. Lett.* **2005**, *86*, 061904−061904−3.
(30) Merkel, P. B.; Dinnocenzo, J. P. *J. Lumin.* **2009**, *129*, 303−306.
(31) Monguzzi, A.; Tubino, R.; Meinardi. *J. Phys. Chem. A* **2009**, *113*, 1171−1174.
(32) Singh-Rachford, T. N.; Lott, J.; Weder, C.; Castellano, F. N. *J. Am. Chem. Soc.* **2009**, *131*, 12007−12014.
(33) Kim, J.-H.; Deng, F.; Castellano, F. N.; Kim, J.-H. *Chem. Mater.* **2012**, *24*, 2250−2252.
(34) Turshatov, A.; Busko, D.; Baluschev, S.; Miteva, T.; Landfester, K. *New J. Phys.* **2011**, *13*, 083035.
(35) Monguzzi, A.; Frigoli, M.; Larpent, C.; Tubino, R.; Meinardi, F. *Adv. Funct. Mater.* **2012**, *22*, 139−143.
(36) Simon, Y. C.; Bai, S.; Sing, M. K.; Dietsch, H.; Achermann, M.; Weder, C. *Macromol. Rapid Commun.* **2012**, *33*, 498−502.
(37) Kang, J. H.; Reichmanis, E. *Angew. Chem., Int. Ed.* **2012**, *51*, 11841−11844.
(38) Reneker, D. H.; Yarin, A. L.; Fong, H.; Koombhongse, S. *J. Appl. Phys.* **2000**, *87*, 4531−4547.
(39) Theron, A.; Zussman, E.; Yarin, A. *Nanotechnology* **2001**, *12*, 384−390.
(40) Hohman, M.M..; Shin, M.; Rutledge, G.; Brenner, M. P. *Phys. Fluids* **2001**, *13*, 2201−2220.
(41) Huang, Z. M.; Zhang, Y. Z.; Kotaki, M.; Ramakrishna, S. *Compos. Sci. Technol.* **2003**, *63*, 2223−2253.
(42) Li, D.; Xia, Y. N. *Adv. Mater.* **2004**, *16*, 1151−1170.
(43) Greiner, A.; Wendorff, J. H. *Angew. Chem., Int. Ed.* **2007**, *46*, 5670−5703.
(44) Crespy, D.; Friedemann, K.; Popa, A. M. *Macromol. Rapid Commun.* **2012**, *33*, 1978−1995.
(45) Stoiljkovic, A.; Ishaque, M.; Justus, U.; Hamel, L.; Klimov, E.; Heckmann, W.; Eckhardt, B.; Wendorff, J. H.; Greiner, A. *Polymer* **2007**, *48*, 3974−3981.
(46) Friedemann, K.; Turshatov, A.; Landfester, K.; Crespy, D. *Langmuir* **2011**, *27*, 7132−7139.
(47) Herrmann, C.; Turshatov, A.; Crespy, D. *ACS Macro Lett.* **2012**, *1*, 907−909.
(48) Lim, J.-M.; Moon, J. H.; Yi, G.-R.; Heo, C.-J.; Yang, S.-M. *Langmuir* **2006**, *22*, 3445−3449.
(49) Horzum, N.; Muñoz-Espí, R.; Glasser, G.; Demir, M. M.; Landfester, K.; Crespy, D. *ACS Appl. Mater. Interfaces* **2012**, *4*, 6338−6345.
(50) Friedemann, K.; Corrales, T.; Kappl, M.; Landfester, K.; Crespy, D. *Small* **2012**, *8*, 144−153.
(51) Lim, J. L.; Yi, G. R.; Moon, J. H.; Heo, C. J.; Yang, S.-M. *Langmuir* **2007**, *23*, 7981−7989.
(52) Dong, B.; Song, H.; Yu, H.; Zhang, H.; Qin, R.; Bai, X.; Pan, G.; Lu, S.; Wang, F.; Fan, L. *J. Phys. Chem. C* **2008**, *112*, 1435−1440.
(53) Hou, Z.; Li, C.; Ma, P.; Li, G.; Cheng, Z.; Peng, C.; Yang, D.; Yang, P.; Lin, J. *Adv. Funct. Mater.* **2011**, *21*, 2356−2365.
(54) Bedford, N. M.; Winget, G. D.; Punnamaraju, S.; Steckl, A. J. *Biomacromolecules* **2011**, *12*, 778−784.
(55) Bansal, P.; Bubel, K.; Agarwal, S.; Greiner, A. *Biomacromolecules* **2012**, *13*, 439−444.
(56) Alay, S.; Göde, F.; Alkan. *Fibers Polym.* **2010**, *11*, 1089−1093.
(57) (a) Zhao, Y.; Fickert, J.; Landfester, K.; Crespy, D. *Small* **2012**, *8*, 2954−2958. (b) Staff, R. H.; Gallei, M.; Mazurowski, M.; Rehahn, M.; Berger, R.; Landfester, K.; Crespy, D. *ACS Nano* **2012**, *6*, 9042−9049.
(58) Massey, L. K. *Permeability Properties of Plastics and Elastomers: A Guide to Packaging and Barrier Materials*; William Andrew: New York, 2003.
(59) Gaume, J.; Wong-Wah-Chung, P.; Rivaton, A.; Gardette, J.-L. *RSC Adv.* **2011**, *1*, 1471−1481.
(60) Turshatov, A.; Busko, D.; Avlasevich, Y.; Miteva, T.; Landfester, K.; Baluschev, S. *ChemPhysChem* **2012**, *13*, 3112−3115.